ARTICLE
Journal of Cellular Biochemistry 112:520–530 (2011)

Journal of Cellular Biochemistry

Examining Rhodopsin Retention in Endoplasmic Reticulum and Intracellular Localization In Vitro and In Vivo by Using Truncated Rhodopsin Fragments

Yuh-Fang Chen,[1,2,3] I-Jong Wang,[2*] Luke L.K. Lin,[2] and Muh-Shy Chen[2]

[1]*Department of Ophthalmology, Taipei County Hospital, Taipei County, Taiwan*

[2]*Department of Ophthalmology, National Taiwan University Hospital, Taipei, Taiwan*

[3]*Graduate Institute of Clinical Medicine, College of Medicine, National Taiwan University, Taipei, Taiwan*

ABSTRACT

More than 100 mutations of rhodopsin have been identified to be associated with retinitis pigmentosa (RP), and mostly autosomal-dominant RP (ADRP). The majority of rhodopsin-associated ADRP is caused by protein misfolding and ER retention. In this study, we aimed to evaluate rhodopsin folding, exiting the ER and intracellular localization through expression of the rhodopsin fragments in COS-1 cells as well as in the transgenic zebrafish. We cloned human rhodopsin cDNA, which was then divided into the N-terminal domain, the C-terminal domain, and the fragment between the N- and C-terminal domains, and examine their intracellular expression in vitro and in vivo. We introduced a point mutation, either F45L or G51V, into this fragment and observed the intracellular localization of these mutants in COS-1 cells and in the zebrafish. The results revealed all of the truncated rhodopsin fragments except for the C-terminal domain and the full-length rhodopsin which had some plasma membrane localization, formed aggregates nearby or within the ER in COS-1 cells; however, the N-terminally truncated rhodopsin fragment, the C-terminal domain, and the full-length rhodopsin could traffic to the ROS in the zebrafish. Besides, the F45L mutation and the G51Vmutation in the rhodopsin fragment between the N- and C-terminal domains produced different effects on the aggresome formation and the intracellular distribution of the mutants both in vivo and in vitro. This current study provides new information about the mutant rhodopsin as well as in treatment of the RP in humans in the future. J. Cell. Biochem. 112: 520–530, 2011.

KEY WORDS: RHODOPSIN; ZEBRAFISH; RETINA

Rhodopsin, a highly specialized G-protein-coupled receptor (GPCR), is the most abundant light-transducing visual pigment integrated in the discs of rod outer segment (ROS). Rhodopsin is synthesized and processed in the endoplasmic reticulum (ER) of the rod inner segment (RIS), and then sent to the ROS through the connecting cilium [Hall et al., 1969]. Since rhodopsin is a typical integral membrane protein, it should have correct topographic arrangement in the ER so that it can undergo proper folding. This depends on a specific signal sequence for a certain fragment of the protein to initiate translocation [Lingappa et al., 1984], and then there should be a stop-transfer sequence to stop the translocation [Yost et al., 1983]. Besides, being a member of the GPCR, rhodopsin shares a number of structural similarities with other GPCRs [Fotiadis et al., 2006]. For example, it consists of a seven-transmembrane domain, an extracellular domain comprised of the N-terminal tail, and a cytoplasmic domain consisting of the C-terminal tail. The N-terminal extracellular domain has been shown to be important for the protein folding and the chromophore binding [Doi and Khorana, 1990]. Mutagenesis in this region resulted in retention of the mutants in the ER and incorrect tertiary structural formation [Anukanth and Khorana, 1994]. The transmembrane domain has many intramolecular interactions that are important in stabilizing the protein structure. Besides, multiple signal and stop-transfer sequences for topogenic translocation within the ER in the transmembrane domains were reported [Audigier et al., 1987]. Furthermore, all seven of the transmembrane segments, together with parts of the extracellular domain, contribute to chromophore binding [Grobner et al., 2000]. Ridge et al. identified some specific amino acid residues responsible for opsin folding, membrane insertion, and assembly in the transmembrane helices through serial works on rhodopsin folding and assembly [Ridge et al., 1995a,b, 1996, 1999; Ridge and Abdulaev,

*Correspondence to: I-Jong Wang, MD, PhD, Department of Ophthalmology, National Taiwan University Hospital, Taiwan, No. 7, Chung-Shan S. Rd., Taipei, Taiwan. E-mail: ijong@ms8.hinet.net

Received 5 January 2010; Accepted 27 October 2010 • DOI 10.1002/jcb.22942 • © 2010 Wiley-Liss, Inc.
Published online 22 November 2010 in Wiley Online Library (wileyonlinelibrary.com).

2000]. The C-terminal cytoplasmic domain of rhodopsin has two major activities: one is the interaction with transducin to initiate the phototransducing cascade [Phillips et al., 1992], and the other is the involvement in protein trafficking [Sung et al., 1994].

More than 100 mutations in the rhodopsin gene have been identified to link with retinitis pigmentosa (RP), and mostly autosomal-dominant RP (ADRP). RP consists of a group of heterogeneous and progressively hereditary diseases with degeneration in photoreceptors due to mutations found in more than 30 genes [Phelan and Bok, 2000]; and it causes severe visual disability in about 1.5 million people worldwide. Characteristically, the patients initially develop night blindness, followed by a gradual constriction of the visual field and eventual loss of central vision [Berson, 1996]. ADRP-associated rhodopsin mutations are generally categorized into two classes according to their biochemical defects in vitro, for example, in cultured COS-7 cells [Sung et al., 1991, 1993]. The majority of rhodopsin mutations, termed class II mutation, result in protein misfolding, the ER retention, low levels of protein expression, and non-functional photopigments on reconstitution with 11-cis-retinal. In contrast, several ADRP mutants behave like the wild-type rhodopsin when expressed in cultured cells. These variants, termed class I mutants, are produced at normal levels and produce a functional photopigment upon 11-cis-retinal reconstitution. In vivo studies proved that most of the class I mutants cluster among the eight amino acids along the C-terminal of the rhodopsin protein, and appear to have trafficking defects to the outer segment of rod photoreceptors [Sandberg et al., 1995].

To investigate the fate of a mutated rhodopsin, whether it can be properly folded in the ER and exit the ER should be evaluated first. If the mutant is misfolded, it accumulates in the ER and leads to imbalance between new protein synthesis and protein processing, resulting in the ''ER stress'' condition [Ron and Walter, 2007]. As a consequence, an integrated intracellular signaling cascade termed the ''unfolded protein reaction (UPR)'' is activated to reestablish the homeostasis and to convert the ER stress. The UPR will slow down new protein formation, and activate chaperones, foldases, as well as proteosome-associated proteins to fasten misfolded protein degradation, the so-called ''ER-associated degradation (ERAD)'' [Schroder and Kaufman, 2005]. Activation of the UPR is a general phenomenon observed in diseases associated with protein misfolding and neuronal dysfunction such as Huntington's disease, Alzheimer's disease, amyotrophic lateral sclerosis, and prion-related disorders [Matus et al., 2008]. Class II rhodopsin-associated ADRP which involves protein misfolding, ER retention and photoreceptor apoptosis is suspected to have similar pathophysiology. To prove this hypothesis, Kang and Ryoo [2009] investigated the genes involved in the ERAD pathway in *Drosophila*, and they demonstrated that ERAD regulators may reduce ER stress and delay retinal degeneration caused by mutant Rh-1 in the *Drosophila* ADRP model.

The knowledge about how different domains of rhodopsin work together to accomplish the assembly process and how mutations of rhodopsin interrupt with this process are important to understand the pathogenesis and the treatment of RP. Hence, we aimed to elucidate the roles of different domains of rhodopsin in protein folding, ER retention, and intracellular distribution by cloning truncated human rhodopsin cDNAs that had been divided into the N-terminal domain, the C-terminal domain, and the fragment between the N- and C-terminal domains, and then transfected them into COS-1 cells. Besides, we also introduced point mutations of F45L and G51V into the fragment between the N- and C-terminal domains to see if their intracellular distribution pattern changes since the classification and the pathogenesis of these two mutations have not been agreed among studies yet [Sung et al., 1993; Hwa et al., 1997; Krebs et al., 2010]. However, since rod photoreceptors are highly specialized, polarized, and compartmentalized phototransducing neurons [Young, 1967], and there are no heterologous cell lines available that exhibit the polarized subcompartmentalization like photoreceptor cells, some errors in protein folding and post-ER trafficking cannot be demonstrated in cultured cells. Therefore, in addition to observing the accumulation of the truncated rhodopsin constructs in COS-1 cells, we also used transgenic zebrafish (*Danio rerio*) to observe their intracellular localization in the highly polarized zebrafish photoreceptor cells. Although the zebrafish model used in our study belongs to the vertebrate family, we still should consider some distinctive feature in the phototransduction visual system including structures, sensitivity, and responsiveness to light among different kinds of vertebrates. However, compared with the invertebrates, obviously more similarities exist in vertebrate phototransduction. For example, stimulation of light leads to hyperpolerization of the photoreceptor in vertebrates while the same event induces depolarization of the cell [Baylor et al., 1979]. Besides, retinal dissociates upon light activation in vertebrates, but this is not observed in invertebrates [Hardie, 1983]. The zebrafish animal model is novel and prolific animal model because of their property of small sizes, high fecundity, rapid growth, and translucent embryos which make the experiments more convenient and economic [Streisinger et al., 1981]. Besides, zebrafish have been proven to be a valuable model organism for study of retinal and photoreceptor associated human diseases due to several reasons. First, the vertebrate species have highly conserved genomes in the visual system so the photoreceptors are genetically close between zebrafish and human beings [Tsujikawa and Malicki, 2004]. Second, large-scale genetic screens using morphological and behavioral criteria have been conducted for a long time, and thousands of mutations in almost every developmental aspect including the visual system have been identified [Haffter et al., 1996]. Third, studies detailing the development and the organization of zebrafish retina and photoreceptor reveal the biological similarity with the human beings [Malicki et al., 1996; Neuhauss et al., 1999].

In the current study, we found that the ability of rhodopsin fragments exiting from ER and the patterns of their intracellular localization are different between in vivo and in vitro. All of the constructs containing rhodopsin fragments showed obvious accumulation in aggresome-like structures and retention in the ER except for the full-length rhodopsin and the C-terminal domain which had some plasma membrane localization in COS-1 cells. On the other hand, the N-terminally truncated rhodopsin fragment, the C-terminal domain and the full-length rhodopsin could direct to the ROS of the zebrafish. Furthermore, point mutations F45L and G51V in rhodopsin fragment between the N- and C-terminal domains had

different effects on the mutant retention and its intracellular distribution both in vivo and in vitro.

MATERIALS AND METHODS

PLASMID CONSTRUCTION

The backbones of the expression plasmids were based on the vector pEGFP-C1 (Clonetech Lab, Inc., Mountain View, CA). EGFP-RHO fusions were created using serial truncations of human rhodopsin cDNA. Unique *Eco*RI and *Bam*HI restriction sites were introduced into the oligonucleotides for cloning into the pEGFP-C1 vector in frame behind the EGFP cDNA. The inserts from serial truncations of human rhodopsin cDNA are summarized in Figure 1, and the primer combinations designed to amplify these different inserts are listed in Table I.

Furthermore, to address possible effects due to the size of EGFP, we established a c-Myc-tagged fragment between the N- and C-terminal domains (a.a. 37–304) using the vector pCMV Tag 3 (Stratagene, La Jolla, CA) and the restriction enzyme sites *Bam*HI and *Eco*RI. The primer combinations were designed as follows: forward 5′-GGATCCCTTCTCCATGCTGGCCGCCTAC-3′, reverse 5′-AATTCCGGACAGGGTTGTAGATGGCGGC-3′. In this vector, the c-Myc-tag is located before the inserted fragment, that is, before a.a. 37.

We also introduced the point mutations G51V and F45L into this construct by site-directed mutagenesis. Mutations were introduced into the pEGFP-human rhodopsin cDNA 204-1007 (a.a. 37–304) construct by replacement of a restriction fragment with synthetic DNA duplexes containing the required codon changes at position 46 or 51. For F45L, the specific mutation was T778C, and for G51V, G797T. The reaction mixture containing wild-type construct, reaction buffer, primers, dNTPs, water, and Pfu DNA polymerase (Stratagene) was used for PCR amplification and the product was then digested with the restriction enzyme *Dpn*I (New England Biolabs, Beverly, MA), leaving only the synthesized strands. The PCR parameters were as follows: pre-denaturation at 95°C for 30 s; followed by 12 cycles of denaturation at 95°C for 10 s, annealing at 55°C for 30 s, and polymerization at 65°C for 150 s; and a final extension step at 65°C for 10 min. The PCR product was then used to transform DH5a competent *E. coli*, and DNA was extracted from selected clones. All of the DNA sequences were confirmed by dideoxynucleotide chain termination.

CELL CULTURE AND TRANSFECTION

African green monkey kidney (COS-1) cells (ATCC CRL-1650) were grown in Dulbecco's modified Eagle's medium (Invitrogen, Carlsbad, CA). All growth media were supplemented with 10% heat-inactivated fetal bovine serum (HyClone Laboratories, Inc., Logan, UT), 1 mM sodium pyruvate, 1 mM sodium glutamate, 0.1 mM MEM non-essential amino acids, 100 U/ml penicillin, and 100 μg/ml streptomycin. COS-1 cells were incubated at 37°C with 5% CO_2. COS-1 cells were seeded at a density of 10,000 cells per well in 6-well plates, and the cells were used for transfect ion after 24 h of settling and adhesion. COS-1 cells were transfected using LipofectAMINE (Invitrogen). The clonal selection medium for selecting stably transfected cells was COS-1 growth medium supplemented with 500 μg/ml Geneticin (G418; Boehringer Mannheim, Mannheim, Germany).

IMMUNOCYTOCHEMISTRY AND LASER CONFOCAL FLUORESCENCE MICROSCOPY OF THE TRANSFECTED COS-1 CELLS

Transfected cells were cultured on sterile coverslips, processed for immunocytochemistry using paraformaldehyde fixation, and imaged using a CCD camera system with excitation/emission filtersets for DAPI, FITC, and TRITC. The primary antibody used to visualize the Golgi apparatus was Golgi (p58) mAb (1:100) (clone 58K-9, Sigma, St. Louis, MO) in antibody diluent, and the secondary antibody was goat anti-mouse-rhodamine (1:100) in PBS. To label

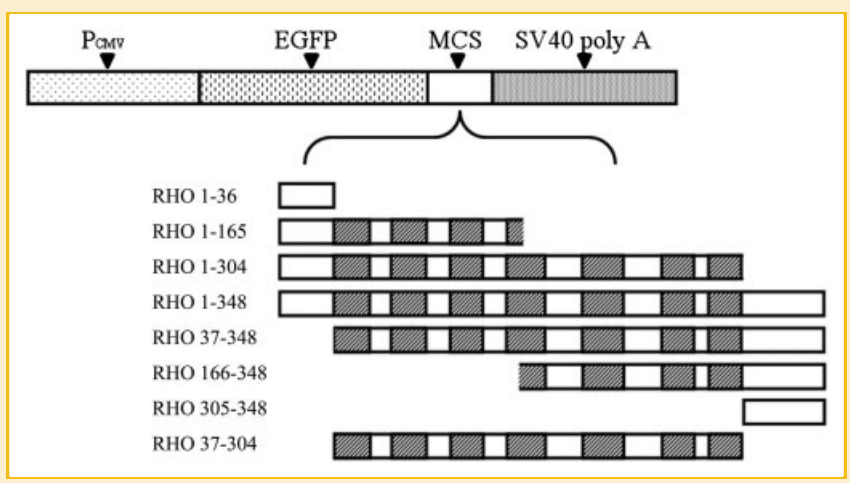

Fig. 1. Schematic diagrams of the EGFP-truncated rhodopsin fusion protein constructs and the inserts of serially truncated human rhodopsin fragments. P_{CMV}: CMV promoter region; MCS: multiple cloning sites; RHO: rhodopsin fragment. The number following RHO stands for the position of the amino acid sequence in the rhodopsin protein. Diagonally striped bars represent the transmembrane domains, and open bars on the left and right sides of the inserts represent the N- and C-terminal domains, respectively; the open bars between the diagonally striped bars represent the cytoplasmic or the extracellular domains.

TABLE I. Primers Used for the Constructs

Amino acid		Primer
1–349	Forward	5′-CGGAATTCCATGAATGGCACAGAAGGCCCT-3′
	Reverse	5′-CGGGATCCCGTTAGGCCGGGGCCACCTG-3′
1–348	Forward	5′-CGGAATTCCATGAATGGCACAGAAGGCCCT-3′
	Reverse	5′-CGGGATCCCGGGCCGGGGCCACCTGGCT-3′
1–304	Forward	5′-CGGAATTCCATGAATGGCACAGAAGGCCCT-3′
	Reverse	5′-CGGGATCCCGGACAGGGTTGTAGATGGCGGC-3′
1–165	Forward	5′-CGGAATTCCATGAATGGCACAGAAGGCCCT-3′
	Reverse	5′-CGGGATCCCGCAGCGCCATGACCCAGGTGAAG-3′
1–36	Forward	5′-CGGAATTCCATGAATGGCACAGAAGGCCCT-3′
	Reverse	5′-CGGGATCCCGCTGCCATGGCTCAGCCAGGTA-3′
37–349	Forward	5′-CGGAATTCCTTCTCCATGCTGGCCGCCTAC-3′
	Reverse	5′-CGGGATCCCGTTAGGCCGGGGCCACCTG-3′
37–304	Forward	5′-CGGAATTCCTTCTCCATGCTGGCCGCCTAC-3′
	Reverse	5′-CGGGATCCCGGACAGGGTTGTAGATGGCGGC-3′
166–349	Forward	5′-CGGAATTCCGCCTGCGCCGCACCCCCA-3′
	Reverse	5′-CGGGATCCCGTTAGGCCGGGGCCACCTG-3′
305–349	Forward	5′-CGGAATTCCATCTATATCATGATGAACAAGCAGTTC-3′
	Reverse	5′-CGGGATCCCGTTAGGCCGGGGCCACCTG-3′

the ER, 250 nM ER-tracker (Blue-White DPX, Invitrogen) was added and incubated at 37°C for 30 min. The labeled cells were transferred to a Zeiss Axiovert inverted microscope (model 410; Carl Zeiss Jena GmbH, Jena, Germany). Fluorescence microscopy of cells was performed using a Zeiss Plan Apo 63X/1.4NA oil immersion lens along with an excitation/emission filterset optimized for EGFP (Chroma Technology Corp., Brattleboro, VT). The microscope, camera, filterwheels, and shutters were controlled by Kinetic Imaging AQM 6 software (Kinetic Imaging, Nottingham, UK).

For the c-Myc tagged constructs, the primary antibody used for the epitope tag was C-Myc (9E10): SC-40 (Santa Cruz Biotechnology, Santa Cruz, CA), and the secondary antibody was Alexa Fluor®488 goat anti-mouse IgG (H + L), A-11001 (Invitrogen) (1:100) in PBS. We used NBD C_6-Ceraminde (Molecular Probes, Inc., Eugene, OR) to label the Golgi apparatus. The primary and the secondary antibodies used to label the ER were oxidoreductase-protein disulfide isomerase (PDI) (E-20) (Santa Cruz Biotechnology), and donkey anti-goat IgG-TR, sc-2783 (Santa Cruz Biotechnology), respectively.

ZEBRAFISH CARE AND EMBRYO MICROINJECTION (TRANSGENESIS)

Zebrafish (*D. rerio*) were raised and utilized for research according to the ARVO Statement for the Use of Animals in Ophthalmic and Vision Research. The linearized plasmids were purified by phenol/chloroform extraction and precipitated with ethanol. Linearized plasmids were diluted to a concentration of 50–100 ng/μl in distilled water and 0.1% phenol red. Embryos were microinjected at the one- to four-cell developmental stage using a microinjector (Drummond Nanoject, Drummond Scientific Co., Broomall, PA).

TISSUE FIXATION AND CONFOCAL FLUORESCENCE MICROSCOPY OF THE TRANSGENIC ZEBRAFISH

The zebrafish was sacrificed on the 10th day of post-fertilization (dpf). Fish eyes were enucleated and fixed in 4% paraformaldehyde in phosphate-buffered saline (PBS), pH 7.0 overnight at 4°C. Following fixation, samples were washed in PBS and incubated with 25% sucrose at 4°C. Samples were oriented in freezing molds in 100% Tissue-Tek OCT medium (Miles) and stored at −20°C until sectioning. Twenty-micron sections were cut on a cryostat, mounted on gelatin-coated slides, and dried for 2–3 h at 25°C. Prior to mounting and observation by confocal microscopy (model 410; Carl Zeiss Jena GmbH), samples were fixed with 4% paraformaldehyde for 5 min, washed with PBS, soaked with 0.4% triton X-100 in PBS for 5 min, and stained with DAPI (1 μg/ml in ddH_2O) for 15 min. Immunostaining for c-Myc was performed as described above. In addition to DAPI, we used an anti-centrin antibody (Anti-Centrin, clone 20H5, Millipore, Billerica, MA) to stain the connecting cilium of the wild-type rod in order to show the boundaries between the RIS and the ROS.

RESULTS

EXPRESSION OF THE EGFP-TRUNCATED RHO FUSION PROTEINS IN COS-1 CELLS

To determine whether different domains of rhodopsin play different roles in protein folding, ER retention, and intracellular localization, we used COS-1 cells to express the EGFP-tagged, N-terminally preserved, truncated rhodopsin constructs and visualized the Golgi and ER with their respective specific antibodies (Fig. 2). Transfection with the constructs without the RHO resulted in a strong EGFP signal in the nucleus and a faint EGFP signal in the cytoplasm. Similarly, the fusion protein containing only the N-terminal domain of rhodopsin (a.a. 1–36) displayed a massive nuclear retention. Then, we lengthened the rhodopsin fragment to contain a.a. 1–165, and found that the localization of the fusion protein shifted out of the nucleus and retained significantly in the ER. We further lengthened the fusion proteins to contain the N-terminal domain and the complete fragment between the N- and C-terminal domains (a.a. 1–304). This truncated fusion protein still form some aggregates in the ER and others distributed non-specifically throughout the cytoplasm. None of these constructs showed Golgi-colocalization patterns, nor did they have plasma membrane association.

In the same way, we examined the intracellular expression of the EGFP-tagged, C-terminally preserved, truncated rhodopsin constructs in COS-1 cells (Fig. 3). Again, all of these constructs (EGFP-RHO a.a. 1–348, 37–348, 166–348, and 305–348) form aggregates nearby or within the ER in different degrees. Among them, the fluorescence signal of full-length rhodopsin (a.a. 1–348) and the C-terminal domain (a.a. 305–348) could both form aggregates and seemed have some plasma membrane localization. Furthermore, we examined the construct of the truncated fusion protein contained the full-length rhodopsin fragment between the N- and C-terminal domains (a.a. 37–304) (Fig. 3), it seemed to form some coarse aggregates within the ER and some small aggregates diffusing in the cytoplasm. No obvious protein colocalization with the Golgi could be detected.

EXPRESSION OF EGFP-TRUNCATED RHO FUSION PROTEINS IN THE ROD CELLS OF ZEBRAFISH

Because no well-differentiated cell models are available that present outer and inner segments similar to photoreceptor cells, we used the zebrafish as an animal model to investigate whether these truncated rhodopsin fragments possessed different determinants in protein

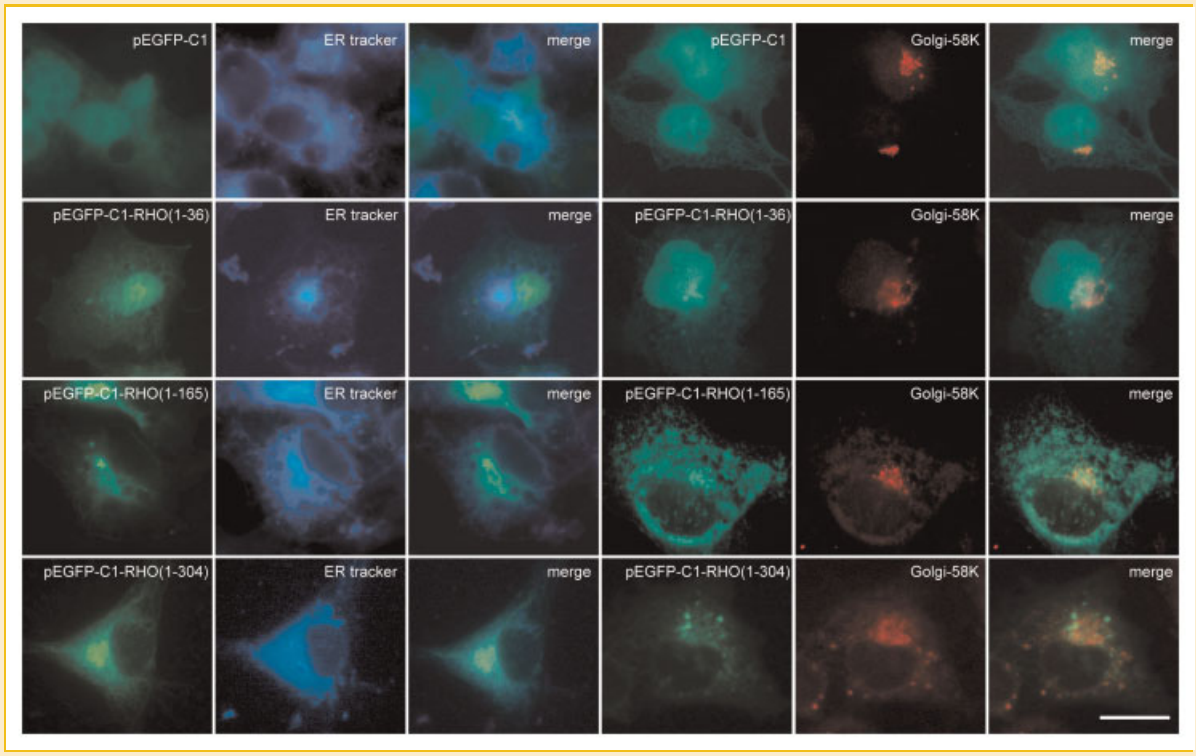

Fig. 2. Expression of the control pEGFP-C1 plasmid (pEGFP-C1) and the EGFP-tagged, N-terminal preserved, truncated rhodopsin (pEGFP-C1-RHO, the number following indicates the inserted fragment of the rhodopsin polypeptide in the fusion protein) in COS-1 cells (*green*). Localization of either the ER (ER tracker, *blue*) or the Golgi (Golgi-58K, *red*) merged with the expression of the above fusion proteins. The signals for the control pEGFP-C1 and pEGFP-C1-RHO (1–36) mainly present in the nucleus. pEGFP-C1-RHO (1–165) is absent from the nucleus and retains significantly in the ER. pEGFP-C1-RHO (1–304) still forms aggregates within and nearby the ER, and also distributes in the cytoplasm non-specifically. There is no obvious colocalization with the Golgi or the plasma membrane. The scale bar stands for 10 μm.

folding, ER retention and intracellular distribution in photoreceptor cells (Fig. 4). First of all, we used an anti-centrin antibody to stain the connecting cilium, and used DAPI to locate the nucleus of rod in the wild-type rod in order to show the boundaries between the RIS and the ROS (Fig. 4, the first icon on the left). Applying this image as a reference, we set the boundaries of RIS in other rods with rhodopsin fragments. Then we evaluated frozen sections of the retinas of transgenic zebrafish expressing EGFP in the rod cells. EGFP signals could be detected in both of the ROS and the RIS in the constructs containing full-length rhodopsin (a.a. 1–348), the N-terminally truncated rhodopsin fragment (a.a. 37–348), and the C-terminal domain (a.a. 305–348). Theoretically, the RIS and ROS are only separated by the connecting cilia so they should be adjacent instead of being separated by a gap. There are two possible explanations for this gap: first, this gap is actually the RIS and that the staining observed in our putative "RIS" may actually be the cone inner segments (CIS) and these data suggest that our constructs may not traffic to the OS in cones, which would be interesting. Second, the gap between RIS and the staining in ROS (represents the EGFP-RHO fusion protein) contains not only the connecting cilium but also the inner part of ROS. That is, we think the EGFP-RHO fusion protein locates in the outer part of ROS. On the other hand, EGFP signals restricted in the RIS in all of the other constructs containing the C-terminal domain and partial fragment between the N- and C-terminal domains (a.a. 166–348), the constructs containing the N-terminally preserved rhodopsin fragment (of a.a. 1–36, 1–165, or 1–304), or the construct containing the full fragment between the N- and C-terminal domain (a.a. 37–304).

EFFECTS OF THE F45L AND G51V MUTATIONS ON TRUNCATED RHODOPSIN EXPRESSION IN VITRO AND IN VIVO

In order to exclude the possibility that EGFP might interfere with folding and intracellular localization of the truncated fusion rhodopsin due to the mass effect, c-Myc-tagged fusion proteins were generated to further evaluate the role of the fragment between the N- and C-terminal domains (a.a. 37–304). Similar to the EGFP-fusion protein, the c-Myc-tagged fragment of a.a. 37–304 formed significant aggregates within ER, and also distributed non-specifically in the cytoplasm in COS-1 cells (Fig. 5). In the zebrafish model, this truncated fusion protein distributed diffusely in the RIS (Fig. 6). The result of in vivo study was in consistent with that of the in vitro study.

We further created a point mutation in this construct, either F45L or G51V, to explore the role of these residues in the protein folding, ER retention, and intracellular distribution of the fragment of a.a. 37–304 in vitro and in vivo. In COS-1 cells, both the F45L and the G51V mutants form aggregates nearby and within the ER (Fig. 5). Nevertheless, the G51V mutant formed larger and coarser aggregates than the F45L mutant. The localization patterns of the mutants were different from that of the wild-type fragment, which

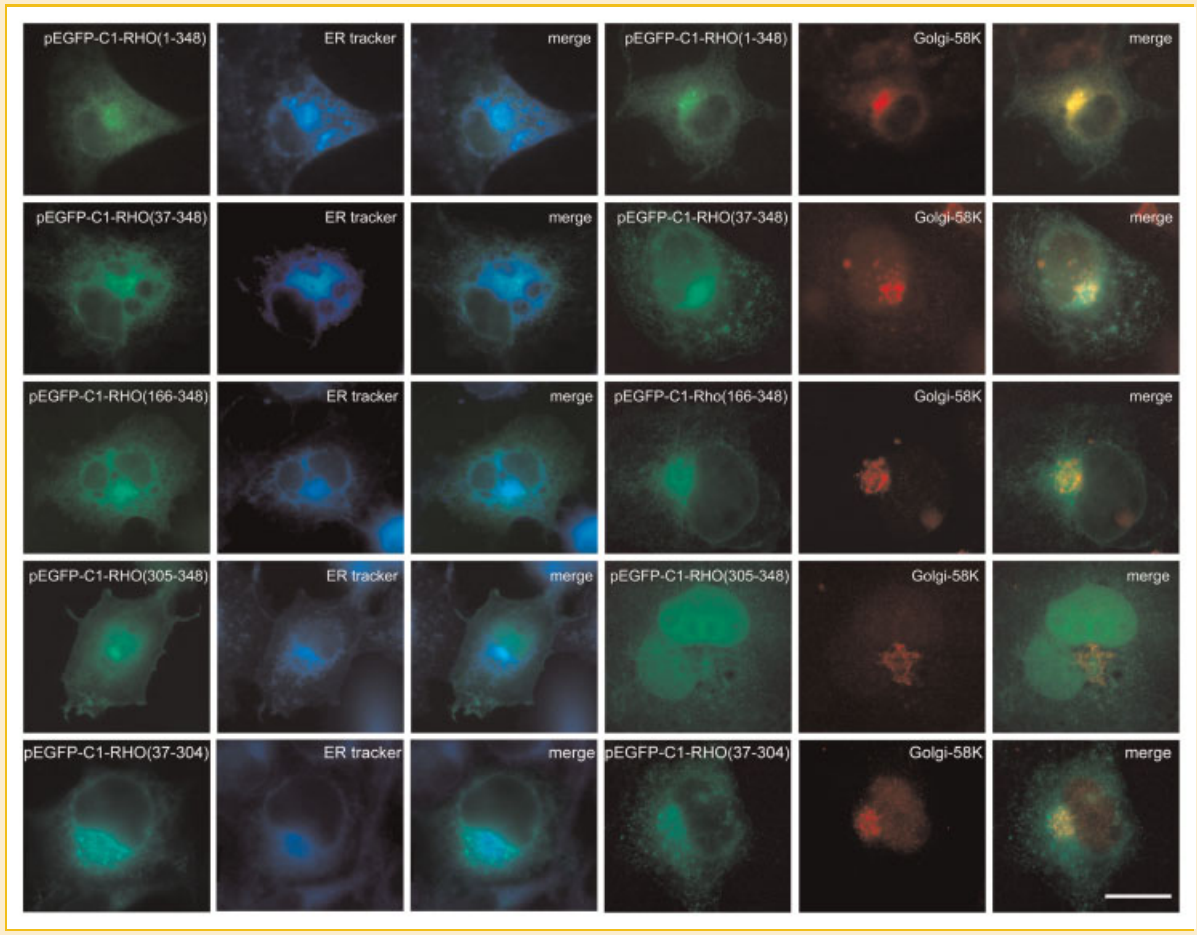

Fig. 3. Expression of the EGFP-tagged, C-terminal preserved, truncated rhodopsin and the fusion proteins containing the fragment between the N- and C- terminal domains in COS-1 cells (*green*) (pEGFP-C1-RHO, the number following indicates the inserted segment of the rhodopsin polypeptide in the fusion protein). Localization of either the ER (ER tracker, *blue*) or the Golgi (Golgi-58K, *red*) merged with the expression of the above fusion proteins. All of the truncated fusion proteins retain significantly within the ER, and some form aggregates in different degrees in the cytoplasm. The aggregates of the full-length rhodopsin (pEGFP-C1-RHO (1–348)) spread widely in the cytoplasm; in addition, it seemed have some non-specific plasma membrane localization. There are still no clear Golgi localization patterns of theses aggregates. The scale bar stands for 10 μm.

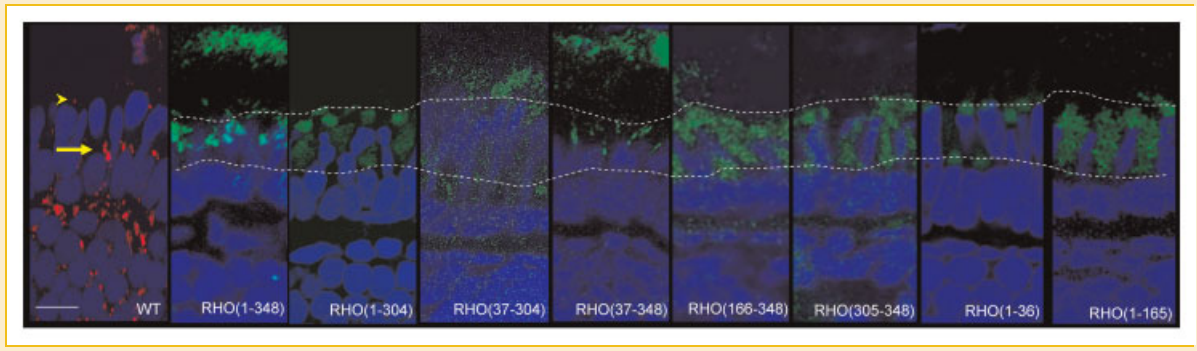

Fig. 4. Expression of the EGFP-truncated rhodopsin fusion proteins (*green*) (pEGFP-C1-RHO, the number following indicates the inserted fragment of the rhodopsin polypeptide in the fusion protein) in rod photoreceptors of zebrafish (the *blue* color is the nucleus stained by DAPI). EGFP signals could be detected in both the ROS and the RIS in the constructs containing either the full-length rhodopsin (pEGFP-C1-RHO (1–348)) or the N-terminal-truncated rhodopsin fragment (pEGFP-C1-RHO (37–348)). EGFP signals were restricted in the RIS in all of the other constructs. The first icon on the left used DAPI and anti-centrin antibody to stain the nucleus (*blue*) and the connecting cilium (*red*), respectively. The arrowhead and the arrow indicate the connecting cilium of the rod cell and that of the cone cell, respectively. The two dash lines demarcate the upper and the lower borders of the RIS. The scale bar represents 5-μm long.

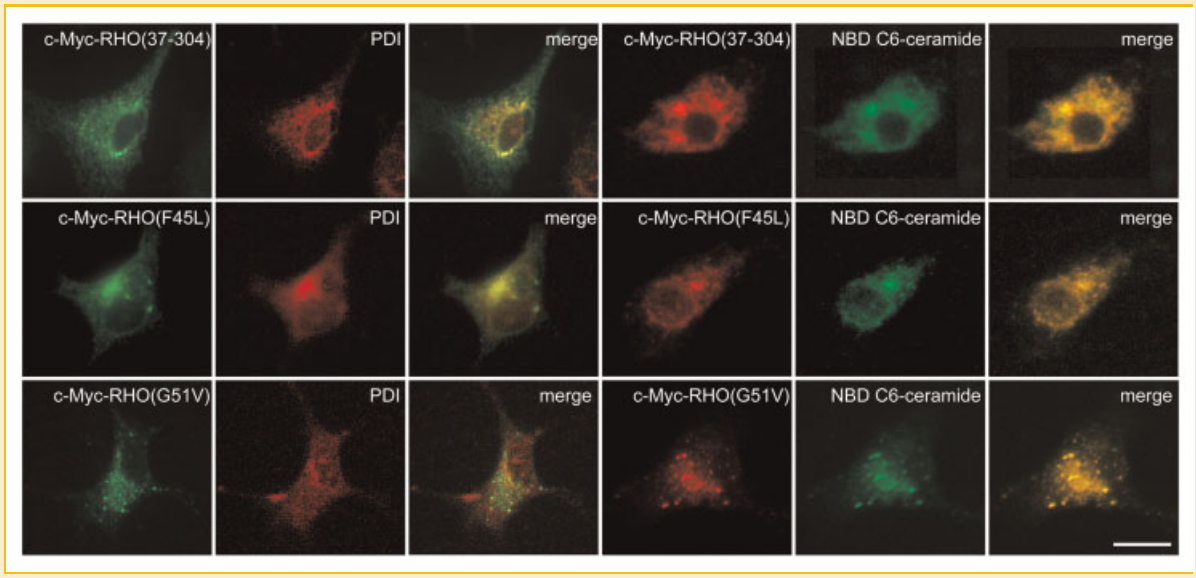

Fig. 5. Expression of the c-Myc-tagged rhodopsin fragment between the N- and C-terminal domains (c-Myc-RHO (37–304)) and its F45L mutant (c-Myc-RHO (F45L)) or the G51V mutant (c-Myc-RHO (G51V)) in COS-1 cells. The *green* signal in the first column indicates the expression of the c-Myc-fusion protein, the *red* signal in the second column indicates the ER (PDI), and the overlap between *green* and *red* appears *yellow* indicating colocalization in the third column. The *red* signal in the fourth column indicates the expression of the c-Myc-fusion protein, the *green* signal in the fifth column indicates the Golgi (NBD C6-ceramide), and similarly, the overlap between *red* and *green* appears *yellow* in the last column. All of the truncated fusion proteins, either the wild type or the mutated ones, form aggregates in the cytoplasm with the greatest concentration in the ER. The aggregates of c-Myc-RHO (37–304), seem more widely and evenly distributed in the cytoplasm than the other two mutants. On the other hand, c-Myc-RHO (G51V) forms most coarse aggregates among the three constructs. There are no Golgi patterns of these aggregates. The scale bar stands for 10 μm.

seemed to distribute more widely in the cytoplasm in addition to the ER retention. There is no Golgi pattern of these aggregates. In rods of the zebrafish, both the G51V and the F45L mutants seemed distribute in the inner part of the RIS while the signal of the wild-type fragment seemed distributed wider than the mutants (Fig. 6).

DISCUSSION

In the present study, we adopted several strategies to improve the validity of the experimental findings. First, the transgenic cDNA was derived by reverse transcription of endogenous human rhodopsin. Because of this, the cloned protein examined in this study was as

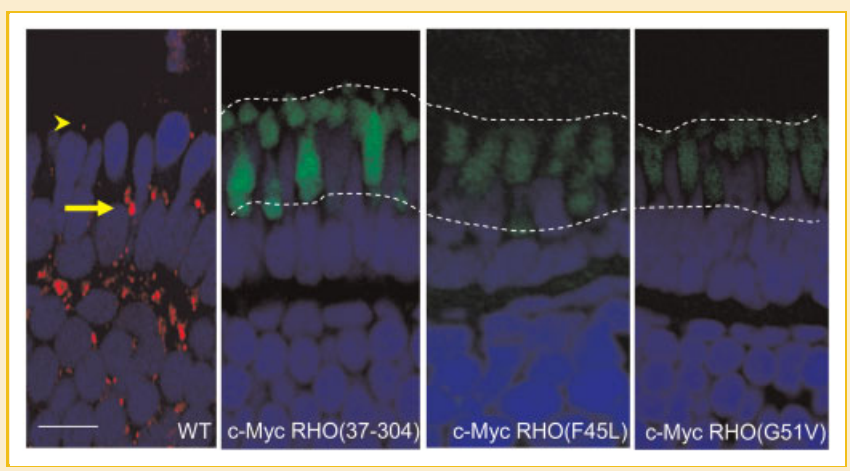

Fig. 6. Expression of the c-Myc-tagged fragment between the N- and C-terminal domains (*green*) (c-Myc-RHO (37–304)) and its F45Lmutant (c-Myc-RHO (F45L)) or the G51V mutant (c-Myc-RHO (G51V)) in rod photoreceptors of zebrafish (*blue*). c-Myc-RHO (37–304) distributes widely in the RIS while c-Myc-RHO (G51V) is predominantly retained in the inner part of the RIS. The range of distribution of c-Myc-RHO (F45L) is in between c-Myc-RHO (37–304) and c-Myc-RHO (G51V). The first icon on the left (the same as Fig. 4) used DAPI and anti-centrin antibody to stain the nucleus (*blue*) and the connecting cilium (*red*), respectively. The arrowhead and the arrow indicate the connecting cilium of the rod cell and that of the cone cell, respectively. The two dash lines demarcate the upper and the lower borders of the RIS. The scale bar represents 5-μm long.

structurally close as possible to that found in human beings. Second, we used a transgenic zebrafish model in addition to the COS-1 cell model to confirm our results. Because COS-1 cells are not polarized and lack the highly differentiated outer and inner segments, the results observed in COS-1 cells might be different from those obtained in the photoreceptors, and could not be directly interpreted as "selective membrane targeting." We expressed the rhodopsin peptides in their native cell type, the rod photoreceptor, in zebrafish, and we believe that the results might be closer to the in vivo situation in humans. All of the truncated rhodopsin containing only the N-terminal domain, C-terminally truncated fragment and partial- or full-length of the fragment between the N- and C-terminal domains retained in the ER both in vivo and in vitro in our study. Using the polypeptide fragment to evaluate its specific role in the protein folding and intracellular expression as done in our study is effective and has been adopted for a long time. Ridge et al. [1995a, 1996] investigated rhodopsin folding and assembly through expressing opsin fragments separated in the intradiscal, transmembrane, and cytoplasmic regions. They demonstrated that all of the opsin fragments seem competent for ER translocation; however, only those separated at key positions in the intradiscal and cytoplasmic regions may form non-covalently linked rhodopsins. Hence, they concluded that the functional assembly of rhodopsin depends on the interactions among multiple folding domains. Ridge et al. [1999] further reported that the transmembrane domain, especially the sixth and the seventh helices, were essential in opsin folding, membrane insertion, and assembly by changing the conformation of the cytoplasmic loops. Focusing on the transmembrane domains, Audigier et al. constructed various opsin mutants, each containing only one transmembrane segment (TMS). They revealed that TMS-1, -2, -4, -5, -6 contain each signal sequence and stop-transfer sequences in variable strength; however, a single TMS does not fold well and exit the ER [Audigier et al., 1987]. Besides, Heymann and Subramaniam [1997] used truncated transmembrane fragments of varying lengths of bovine rhodopsin and found that all of the polypeptides that contained partial transmembrane fragments were retained in the ER. Our observation was in concordance with theirs that the fragment between the N- and C-terminal domains retained in the ER.

In the current study, we showed that misfolded proteins formed aggresome-like material in the COS-1 cells but not in photoreceptors. Several studies investigating the intracellular fate of the mutant rhodopsin in vitro agree our results. Saliba et al. examine P23H and K296E mutated opsin processing in COS-7 cells. They found that the mutant protein forms aggresome-like aggregates instead of accumulating in the Golgi. They suggested that the aggregates may recruit specific opsin-binding proteins like Tctex or the C-terminal-binding sorting factors, and thus interrupt the targeting of the normal proteins to the outer segment of the photoreceptor. Besides, the aggregation may also induce cellular stress and stimulate an unfolded protein response, and then compromise photoreceptor viability [Saliba et al., 2002]. Illing et al. [2002] evaluated the expression of P23H in HEK cells, and they reported that the mutant which is a substrate for ubiquitin-dependent degradation may form aggresomes and impair the function of the ubiquitin proteosome system, and thus becomes a toxic gain of function in the pathogenesis of class II mutations. On the other hand, in vivo studies had very diverse results about the fate of misfolded proteins due to different models availed. For example, while rhodopsin P23H was misfolded and retained in the RIS without aggresomes formation in a *Xenopus laevis* model [Tam and Moritz, 2006], rhodopsin P23H distributed predominantly in the ROS in transgenic mice [Wu et al., 1998]. Since biological diversity among animals is an important environmental factor to gain different experimental results, it is valuable to establish new animal models such as zebrafish for another chance to understand human diseases and to provide new therapies.

It was not surprising that full-length rhodopsin can traffic to the plasma membrane both in vivo and in vitro in our study. The result that rhodopsin fragment containing the C-terminal domain alone showed some plasma membrane localization in addition to aggregates formation both in vivo and in vitro was also predictable since protein trafficking function of the C-terminal domain in rhodopsin has been well documented with the following evidences: First, all mutations clustered in the C-terminal in human rhodopsin-related ADRP have protein trafficking defects [Sung and Tai, 2000]. Second, defects in rhodopsin trafficking to the ROS in vivo or in vitro carrying mutations in this region [Sung et al., 1994; Deretic et al., 1998]. Third, the C-domain can interact directly with the cargo-binding subunit of the cytoplasmic dynein light-chain Tctex-1, which appears to control the targeting of rhodopsin to the ROS [Tai et al., 1999]. Furthermore, Deretic et al. [2005] reported that the rhodopsin cytoplasmic terminus can bind specifically to a small GTPase, ADP-ribosylation factor 4, which is critical for the sorting of post-Golgi carriers to the ROS.

It is interesting and beyond our expectations that the expressions of the N-terminally truncated fragment were different between in vivo and in vitro in our study. In COS-1 cells, this fragment seemed totally retained in the ER, but it could traffic to the ROS. There are two explanations for this finding. First, the ER may have better ability to fold proteins in photoreceptors, produce less abnormal proteins and aggregates, or have larger capacity to clear misfolded proteins than in COS-1 cells. Similar findings had been documented that the inclusion bodies was much less in the RP patients than in other neurodegeneration diseases in the central nervous system or in cultured cells like HEK cells or COS cells [Flannery et al., 1989; Johnston et al., 2000]. Second, the N-terminally truncated rhodopsin may fold stably so that it can exit the ER and does not induce ER stress or the UPR so that it does not form aggregates. In fact, the N-terminally truncated rhodopsin from different sources also had different fates in the same animal model. Tam and Moritz [2007] reported that N-terminally truncated P23H rhodopsin from human and bovine exited the ER and was transported to the ROS in a transgenic *X. laevis* model; however, N-terminally truncated *X. laevis* P23H retained in the ER and did not show any rescue of retinal degeneration in the same model.

To clarify the effect of G51V and F45L on processing and folding of the transmembrane domain of rhodopsin, we introduced either G51V or F45L into the fragment between the N- and C-terminal domains of rhodopsin (a.a. 37–304). Our study revealed that both the mutations increased the tendency of protein retention in the ER and limited their intracellular distribution. However, there were pitfalls

in this design that since the rhodopsin fragment (a.a. 37–304) itself has already been misfolded and retained in the ER due to lacking of glycosylation sites, the effect of the point mutation per se would be hard to measure alone. Besides, we noticed that the pattern of aggregation was different between G51V and F45L, that is, the G51V mutant formed larger and coarser aggregates than the F45L mutant. This was an interesting finding although the pathophysiological mechanism and its implication are unclear. To improve the study design, we would introduce the point mutations in full-length protein, and then quantify the size, number or mobility precisely to elucidate the different behavior between F4L and G51V in our further investigation. Hwa et al. studied the functions of the transmembrane regions in the packing of helices and the folding of the protein into a tertiary structure by performing site-directed mutagenesis. They reported that all of the mutations in this region including G51V caused partial misfolding of the opsin and strong signs of ER retention as observed by the UV/visible absorption characteristics, although they showed that not all mutations cause equally severe effects on misfolding and ER retention [Hwa et al., 1997]. Bosch et al. [2003] elucidated pathophysiological mechanisms of the G51V mutation and found that the interhelical protein packing would be disrupted by a steric hindrance of the Val-300 side chain and a disturbance of the local helix residue Pro-303, and thus causes instability of the mutant. Furthermore, Krebs et al. [2010] reclassified the G51V mutation into class III because it was misfolded compared to the wild-type rhodopsin. However, all of the above studies were carried out in vitro, such as in COS-1 cells, rather than in highly subcompartmentalized photoreceptor cells.

Furthermore, the effects of EGFP on the folding and trafficking of the fusion protein should be concerned since EGFP is much larger than the truncated rhodopsin fragments established in our study. In the study of the cellular fate of rhodopsin by Saliba et al. [2002], they used the vector pEGFP-N1 with a GFP tag fused to the C-terminus of the opsin, and they demonstrated that the GFP tag to the C-terminus of opsin increased the possibility of aggresome formation. Moritz et al. [2001] also demonstrated that opsin-GFP could be folded well and produce functional visual pigment, but misfolding possibility is higher than the opsin without tagging. Nevertheless, the pEGFP-C1 vector used in our study has a GFP tag to the N-terminus of opsin. Similarly, we used the vector pCMV Tag 3 to establish a c-Myc-tagged-rhodopsin fragment (a.a. 37–304) construct, and the c-Myc-tag also locates at the N-terminus of the opsin fragment. Hence, the constructs designed in our study might have less influence on protein folding theoretically. Furthermore, A pEGFP-C1 vector was used to create C-terminal truncations constructs with or without modifications in Tamet's study to identify the outer segment targeting signal in the C-terminus of rhodopsin [Tam et al., 2000]. Their results supported the notion that the fate of the fusion protein was specific to the rhodopsin fragments but not due to the effect of EGFP. In addition to EGFP, Sung et al. [1993] chose the smaller mAb B6-30, which can recognize an epitope near the amino terminus of rhodopsin, to localize the protein. And they found that both tagged proteins exhibited a similar intracellular distribution. To exclude the mass effect of EGFP, we used c-Myc instead of EGFP to produce fusion proteins containing the fragment between the N- and C-terminal domains with either a F45L or a G51V mutation in both COS-1 cells and in zebrafish photoreceptors. Our results revealed similar ER retention and intracellular distributions between EGFP-fusion proteins and c-Myc-tagged fusion proteins. Hence, we concluded that EGFP had no obvious effect on protein folding and distribution in our study.

One of the weak points of our study was that we used the non-specific CMV promoter instead of tissue-specific promoters to drive the plasmid; thus, the RIS could only be suggested by its morphology. There are several possible resolutions to this problem. First, we may use rod-specific promoters to drive the plasmids. Second, we may stain subtypes of opsins like RH1 in rods, SWS-1, SWS-2, MWS/LWS, and RH2 in cones [Yokoyama, 2000a,b]. Third, we may utilize rod- or cone-specific antibodies such as the monoclonal antibody, FRet43, for an uncharacterized plasma membrane epitope on double cone photoreceptors, or another monoclonal antibody, ROSl, for an uncharacterized epitope on ROS [Raymond et al., 1995]. Furthermore, immunoenzyme or immunofluorescence double staining technology is certainly the way of choice to co-localize two antigens like a specific plasmid and an epitope on ROS simultaneously to make sure their localization and to enhance the validity of the retinal staining.

We concluded that the ability of truncated rhodopsin fragments exiting the ER and the patterns of their intracellular localization are different between in vivo and in vitro. In the COS-1 cell, only the C-terminal domain and the full-length rhodopsin showed some plasma membrane localization in addition to ER retention. In the zebrafish, both of the C-terminal domain and the N-terminally truncated rhodopsin fragment, as well as the full-length of rhodopsin, could traffic to the ROS. Furthermore, point mutations F45L and G51V in rhodopsin fragment between the N- and C-terminal domains did not have similar effect on retention and intracellular distribution of the mutants both in vivo and in vitro. This current study provides new information about mutant rhodopsin in a zebrafish model compared with COS-1 cells, and is valuable in better understanding about rhodopsin as well as the RP in humans. Our further study will focus on the mechanisms of the N-terminally truncated rhodopsin folding in the ER. This effort may give us a new hope in the treatment of the RP in humans.

REFERENCES

Anukanth A, Khorana HG. 1994. Structure and function in rhodopsin. Requirements of a specific structure for the intradiscal domain. J Biol Chem 269:19738–19744.

Audigier Y, Friedlander M, Blobel G. 1987. Multiple topogenic sequences in bovine opsin. Proc Natl Acad Sci USA 84:5783–5787.

Baylor DA, Lamb TD, Yau KW. 1979. The membrane current of single rod outer segments. J Physiol 288:589–611.

Berson EL. 1996. Retinitis pigmentosa: Unfolding its mystery. Proc Natl Acad Sci USA 93:4526–4528.

Bosch L, Ramon E, Del Valle LJ, Garriga P. 2003. Structural and functional role of helices I and II in rhodopsin. A novel interplay evidenced by mutations at Gly-51 and Gly-89 in the transmembrane domain. J Biol Chem 278: 20203–20209.

Deretic D, Schmerl S, Hargrave PA, Arendt A, McDowell JH. 1998. Regulation of sorting and post-Golgi trafficking of rhodopsin by its C-terminal sequence QVS(A)PA. Proc Natl Acad Sci USA 95:10620–10625.

Deretic D, Williams AH, Ransom N, Morel V, Hargrave PA, Arendt A. 2005. Rhodopsin C terminus, the site of mutations causing retinal disease, regulates trafficking by binding to ADP-ribosylation factor 4 (ARF4). Proc Natl Acad Sci USA 102:3301–3306.

Doi TMR, Khorana HG. 1990. Role of the intradiscal domain in rhodopsin assembly and function. Proc Natl Acad Sci USA 87:4991–4995.

Flannery JG, Farber DB, Bird AC, Bok D. 1989. Degenerative changes in a retina affected with autosomal dominant retinitis pigmentosa. Invest Ophthalmol Vis Sci 30:191–211.

Fotiadis D, Jastrzebska B, Philippsen A, Muller DJ, Palczewski K, Engel A. 2006. Structure of the rhodopsin dimer: A working model for G-protein-coupled receptors. Curr Opin Struct Biol 16:252–259.

Grobner G, Burnett IJ, Glaubitz C, Choi G, Mason AJ, Watts A. 2000. Observations of light-induced structural changes of retinal within rhodopsin. Nature 405:810–813.

Haffter P, Granato M, Brand M, Mullins MC, Hammerschmidt M, Kane DA, Odenthal J, van Eeden FJ, Jiang YJ, Heisenberg CP, Kelsh RN, Furutani-Seiki M, Vogelsang E, Beuchle D, Schach U, Fabian C, Nusslein-Volhard C. 1996. The identification of genes with unique and essential functions in the development of the zebrafish, *Danio rerio*. Development 123:1–36.

Hall MO, Bok D, Bacharach AD. 1969. Biosynthesis and assembly of the rod outer segment membrane system. Formation and fate of visual pigment in the frog retina. J Mol Biol 45:397–406.

Hardie RC. 1983. Projection and connectivity of sex-specific photoreceptors in the compound eye of the male housefly (Musca domestica). Cell Tissue Res 233:1–21.

Heymann JA, Subramaniam S. 1997. Expression, stability, and membrane integration of truncation mutants of bovine rhodopsin. Proc Natl Acad Sci USA 94:4966–4971.

Hwa J, Garriga P, Liu X, Khorana HG. 1997. Structure and function in rhodopsin: Packing of the helices in the transmembrane domain and folding to a tertiary structure in the intradiscal domain are coupled. Proc Natl Acad Sci USA 94:10571–10576.

Illing ME, Rajan RS, Bence NF, Kopito RR. 2002. A rhodopsin mutant linked to autosomal dominant retinitis pigmentosa is prone to aggregate and interacts with the ubiquitin proteasome system. J Biol Chem 277:34150–34160.

Johnston JA, Dalton MJ, Gurney ME, Kopito RR. 2000. Formation of high molecular weight complexes of mutant Cu, Zn-superoxide dismutase in a mouse model for familial amyotrophic lateral sclerosis. Proc Natl Acad Sci USA 97:12571–12576.

Kang MJ, Ryoo HD. 2009. Suppression of retinal degeneration in Drosophila by stimulation of ER-associated degradation. Proc Natl Acad Sci USA 106:17043–17048.

Krebs MP, Holden DC, Joshi P, Clark CL III, Lee AH, Kaushal S. 2010. Molecular mechanisms of rhodopsin retinitis pigmentosa and the efficacy of pharmacological rescue. J Mol Biol 395:1063–1078.

Lingappa VR, Chaidez J, Yost CS, Hedgpeth J. 1984. Determinants for protein localization: Beta-lactamase signal sequence directs globin across microsomal membranes. Proc Natl Acad Sci USA 81:456–460.

Malicki J, Neuhauss SC, Schier AF, Solnica-Krezel L, Stemple DL, Stainier DY, Abdelilah S, Zwartkruis F, Rangini Z, Driever W. 1996. Mutations affecting development of the zebrafish retina. Development 123:263–273.

Matus S, Lisbona F, Torres M, Leon C, Thielen P, Hetz C. 2008. The stress rheostat: An interplay between the unfolded protein response (UPR) and autophagy in neurodegeneration. Curr Mol Med 8:157–172.

Moritz OL, Tam BM, Papermaster DS, Nakayama T. 2001. A functional rhodopsin-green fluorescent protein fusion protein localizes correctly in transgenic *Xenopus laevis* retinal rods and is expressed in a time-dependent pattern. J Biol Chem 276:28242–28251.

Neuhauss SC, Biehlmaier O, Seeliger MW, Das T, Kohler K, Harris WA, Baier H. 1999. Genetic disorders of vision revealed by a behavioral screen of 400 essential loci in zebrafish. J Neurosci 19:8603–8615.

Phelan JK, Bok D. 2000. A brief review of retinitis pigmentosa and the identified retinitis pigmentosa genes. Mol Vis 6:116–124.

Phillips WJ, Wong SC, Cerione RA. 1992. Rhodopsin/transducin interactions. II. Influence of the transducin-beta gamma subunit complex on the coupling of the transducin-alpha subunit to rhodopsin. J Biol Chem 267:17040–17046.

Raymond PA, Barthel LK, Curran GA. 1995. Developmental patterning of rod and cone photoreceptors in embryonic zebrafish. J Comp Neurol 359:537–550.

Ridge KD, Abdulaev NG. 2000. Folding and assembly of rhodopsin from expressed fragments. Methods Enzymol 315:59–70.

Ridge KD, Lee SS, Abdulaev NG. 1996. Examining rhodopsin folding and assembly through expression of polypeptide fragments. J Biol Chem 271:7860–7867.

Ridge KD, Lee SS, Yao LL. 1995a. In vivo assembly of rhodopsin from expressed polypeptide fragments. Proc Natl Acad Sci USA 92:3204–3208.

Ridge KD, Lu Z, Liu X, Khorana HG. 1995b. Structure and function in rhodopsin. Separation and characterization of the correctly folded and misfolded opsins produced on expression of an opsin mutant gene containing only the native intradiscal cysteine codons. Biochemistry 34:3261–3267.

Ridge KD, Ngo T, Lee SS, Abdulaev NG. 1999. Folding and assembly in rhodopsin. Effect of mutations in the sixth transmembrane helix on the conformation of the third cytoplasmic loop. J Biol Chem 274:21437–21442.

Ron D, Walter P. 2007. Signal integration in the endoplasmic reticulum unfolded protein response. Nat Rev Mol Cell Biol 8:519–529.

Saliba RS, Munro PM, Luthert PJ, Cheetham ME. 2002. The cellular fate of mutant rhodopsin: Quality control, degradation and aggresome formation. J Cell Sci 115:2907–2918.

Sandberg MA, Weigel-DiFranco C, Dryja TP, Berson EL. 1995. Clinical expression correlates with location of rhodopsin mutation in dominant retinitis pigmentosa. Invest Ophthalmol Vis Sci 36:1934–1942.

Schroder M, Kaufman RJ. 2005. The mammalian unfolded protein response. Annu Rev Biochem 74:739–789.

Streisinger G, Walker C, Dower N, Knauber D, Singer F. 1981. Production of clones of homozygous diploid zebra fish (*Brachydanio rerio*). Nature 291:293–296.

Sung CH, Davenport CM, Nathans J. 1993. Rhodopsin mutations responsible for autosomal dominant retinitis pigmentosa. Clustering of functional classes along the polypeptide chain. J Biol Chem 268:26645–26649.

Sung CH, Makino C, Baylor D, Nathans J. 1994. A rhodopsin gene mutation responsible for autosomal dominant retinitis pigmentosa results in a protein that is defective in localization to the photoreceptor outer segment. J Neurosci 14:5818–5833.

Sung CH, Schneider BG, Agarwal N, Papermaster DS, Nathans J. 1991. Functional heterogeneity of mutant rhodopsins responsible for autosomal dominant retinitis pigmentosa. Proc Natl Acad Sci USA 88:8840–8844.

Sung CH, Tai AW. 2000. Rhodopsin trafficking and its role in retinal dystrophies. Int Rev Cytol 195:215–267.

Tai AW, Chuang JZ, Bode C, Wolfrum U, Sung CH. 1999. Rhodopsin's carboxy-terminal cytoplasmic tail acts as a membrane receptor for cytoplasmic dynein by binding to the dynein light chain Tctex-1. Cell 97:877–887.

Tam BM, Moritz OL. 2006. Characterization of rhodopsin P23H-induced retinal degeneration in a *Xenopus laevis* model of retinitis pigmentosa. Invest Ophthalmol Vis Sci 47:3234–3241.

Tam BM, Moritz OL. 2007. Dark rearing rescues P23H rhodopsin-induced retinal degeneration in a transgenic *Xenopus laevis* model of retinitis pigmentosa: A chromophore-dependent mechanism characterized by pro-

duction of N-terminally truncated mutant rhodopsin. J Neurosci 27:9043–9053.

Tam BM, Moritz OL, Hurd LB, Papermaster DS. 2000. Identification of an outer segment targeting signal in the COOH terminus of rhodopsin using transgenic *Xenopus laevis*. J Cell Biol 151:1369–1380.

Tsujikawa M, Malicki J. 2004. Genetics of photoreceptor development and function in zebrafish. Int J Dev Biol 48:925–934.

Wu TH, Ting TD, Okajima TI, Pepperberg DR, Ho YK, Ripps H, Naash MI. 1998. Opsin localization and rhodopsin photochemistry in a transgenic mouse model of retinitis pigmentosa. Neuroscience 87:709–717.

Yokoyama S. 2000a. Color vision of the coelacanth (Latimeria chalumnae) and adaptive evolution of rhodopsin (RH1) and rhodopsin-like (RH2) pigments. J Hered 91:215–220.

Yokoyama S. 2000b. Molecular evolution of vertebrate visual pigments. Prog Retin Eye Res 19:385–419.

Yost CS, Hedgpeth J, Lingappa VR. 1983. A stop transfer sequence confers predictable transmembrane orientation to a previously secreted protein in cell-free systems. Cell 34:759–766.

Young RW. 1967. The renewal of photoreceptor cell outer segments. J Cell Biol 33:61–72.